Decoupling peroxyacetyl nitrate from ozone in Chinese outflows observed at Gosan Climate Observatory

Jihyun Han[1*], Meehye Lee[1], Xiaona Shang[1], Gangwoong Lee[2], Louisa K. Emmons[3]

[1]Department of Earth and Environmental Sciences, Korea University, Seoul, Republic of Korea

[2]Department of Environmental Science, Hankuk University of Foreign Studies, Yongin, Republic of Korea

[3]Atmospheric Chemistry Observations and Modeling Laboratory, National Center for Atmospheric Research (NCAR), Boulder, CO, USA

*now at: Korea Environment Institute, Sejong, Republic of Korea

Correspondence to: M. Lee (meehye@korea.ac.kr)

Submitted to Atmospheric Chemistry and Physics

December 2016

Abstract

We measured peroxyacetyl nitrate (PAN) and other reactive species such as O_3, NO_2, CO, and SO_2 with aerosols including mass, organic carbon (OC), and elemental carbon (EC) in $PM_{2.5}$ and K^+ in $PM_{1.0}$ at Gosan Climate Observatory in Korea (33.17°N, 126.10°E) during October 19 to November 6, 2010. PAN was determined through fast gas chromatography with luminol chemiluminescence detection at 425 nm every 2 min. The PAN mixing ratios ranged from 0.1 (detection limit) to 2.4 ppbv with a mean of 0.6 ppbv. For all measurements, PAN was unusually better correlated with $PM_{2.5}$ (Pearson correlation coefficient, $\gamma = 0.79$) than with O_3 ($\gamma = 0.67$). In particular, the O_3 level was highly elevated with SO_2 at midnight, along with a typical midday peak when air was transported rapidly from the Beijing areas. The PAN enhancement was most noticeable during the occurrence of haze under stagnant conditions. In Chinese outflows slowly transported over the Yellow Sea, PAN gradually increased up to 2.4 ppbv at night, in excellent correlation with a concentration increase of $PM_{2.5}$ OC and EC, $PM_{2.5}$ mass, and $PM_{1.0}$ K^+. The high K^+ concentration and OC/EC ratio indicated that the air mass was impacted by biomass combustion. This study highlights PAN decoupling with O_3 in Chinese outflows and suggests PAN as a useful indicator for diagnosing continental outflows and assessing their perturbation on regional air quality in northeast Asia.

Key words: PAN, O_3, $PM_{2.5}$, Chinese outflow, Haze, Biomass combustion

1. Introduction

At the surface, ozone is primarily photochemically produced, and the contribution from the stratosphere is generally small. Ozone is formed through reactions of various precursors such as CO, CH_4, volatile organic compounds (VOCs), and NO_x (e.g., Brasseur et al., 1999; Jacob, 2000; Nielsen et al., 1981). Likewise, peroxyacetyl nitrate (PAN) is a secondary product of urban air pollution and a significant oxidant in the atmosphere (e.g., Hansel and Wisthaler, 2000; La Franchi et al., 2009; Lee et al., 2012; Liu et al., 2010; Roberts et al., 2007). PAN is solely produced by the photochemical reaction between the peroxyacetyl radical and nitrogen dioxide, and the peroxyacetyl radical is derived from the OH oxidation or photolysis of VOCs such as acetaldehyde, methylglyoxal, and acetone (e.g., Fischer et al., 2014; La Franchi et al., 2009; Lee et al., 2012). For this reason, PAN is a very useful indicator of photochemical air pollution. As thermal decomposition is a major PAN sink in the troposphere (Beine et al., 1997; Jacob, 2000; Kenley and Hendry, 1982; Talukdar et al., 1995), the lifetime of PAN depends on temperature. For example, the PAN lifetime is ~5 years at −26°C and 1 h at 20°C (Fischer et al., 2010; Zhang et al., 2011). At high altitudes above ~7 km, photolysis becomes the most important loss process for PAN (Talukdar, et al., 1995). Because of low solubility, PAN is not prone to atmospheric removal, thereby being more efficiently transported to the free troposphere (e.g., Zhu et al., 2017). Thus, PAN can be an indicator of NO_y concentration in the free troposphere and a guide for the long-range transport of NO_x in remote regions (Jacob, 1999).

In the past decades, PAN was measured not only in urban areas (Aneja et al., 1999; Gaffney et al., 1999; Grosjean et al., 2002; Lee et al., 2008; Tanimoto et al., 1999; Zhang et al., 2014) but also in background regions (Fischer et al., 2011; Kanaya et al., 2007; Lee et al.,

71 2012; Tanimoto et al., 2002), onboard aircraft (Tereszchuk et al., 2013), and ships (Roberts et

72 al., 2007). PAN concentrations were in the range of a few ppbv in urban areas close to VOCs

73 and NO_x sources (Lee et al., 2008; Zhang et al., 2011). In the most remote regions, PAN

74 concentrations were generally in the range of a few pptv (Gallagher et al., 1990; Mills et al.,

75 2007; Muller and Rudolph, 1992; Staudt et al., 2003).

76 Although NO_x concentration has recently declined in China (Gu et al., 2013; Liu et al.,

77 2016a; Krotkov et al., 2016), NO_x and VOCs have gradually increased in East Asia,

78 particularly China during the last couple of decades (Akimoto, 2003; Liu et al., 2010; Ohara

79 et al., 2007; Zhao et al., 2013). It led to an increase in the concentrations of photochemical

80 byproducts such as PAN and O_3 not only in East Asia (Liu et al., 2010; Wang et al., 2010;

81 Zhang et al., 2009; Zhang et al., 2011; Zhang et al., 2014) but also in North America (Fischer

82 et al., 2010; Fischer et al., 2011; Jaffe et al., 2007; Zhang et al., 2008). These results were

83 also demonstrated by the GEOS-Chem model (Zhang et al., 2008). In addition to urban

84 plumes, PAN was reported to be enhanced by biomass combustion (Alvarado et al., 2010;

85 Coheur et al., 2007; Zhu et al., 2015; Zhu et al., 2017), such as open burning and use of

86 biofuel, which is used to take place often in China after crop harvesting (Cao et al., 2006;

87 Duan et al., 2004). Recent satellite studies have also observed the increased PAN in plumes

88 associated with anthropogenic emissions in eastern China and boreal fires in Siberia (Zhu et

89 al., 2015; Zhu et al., 2017). In this context, PAN is a useful tracer for estimating the impact of

90 Chinese outflows on regional air quality in the northern Pacific region.

91 Gosan Climate Observatory (GCO) is an ideal place to monitor Asian outflows and their

92 transformation and to estimate their impact on air quality over the northern Pacific region

93 (Lee et al., 2007; Lim et al., 2012). In the present study, PAN was first measured

94 continuously at GCO to characterize its variation and source in relation to O_3 and to

95 understand the influence of Chinese outflows on the regional air quality.

96

97 **2. Experiments**

98

99 PAN measurements were conducted at GCO (33.17°N, E126.10°E) on Jeju Island from

100 October 19 to November 6, 2010. GCO is located on a cliff at the western edge of Jeju Island.

101 PAN was determined through fast gas chromatography (GC) with luminol

102 chemiluminescence detection, which is described in detail elsewhere (Gaffney et al., 1998;

103 Lee et al., 2008; Marley et al., 2004). Here, we briefly describe the measurement method.

104 Ambient air was pumped through a 1.6-m PFA tubing (1/4 inch outer diameter) from the

105 roof of the two-story container into a six-port injection valve (Cheminert C22, Valco

106 Instruments (Houston, TX, USA)) at 100 ml/min controlled by Mass flow controller (Lee et

107 al., 2012; Lee et al., 2008). The residence time of the inlet was less than 2 seconds. PAN and

108 NO_2 (and peroxypropyl nitrate (PPN) if present) were separated along a 10-m capillary GC

109 column (DB-1, J&W Scientific, Folsom, CA, USA), whose end was connected to a luminol

110 cell where the column effluent reacted with luminol, giving off luminescent light (Lee et al.,

111 2008; Lee et al., 2012). The concentrations of PAN and other species were determined from

112 the chemiluminescence signals detected by a gated photon counter (HC135-01, Hamamatsu,

113 Bridgewater, NJ, USA) at 425 nm, which was set at 800 V and operated at room temperature

114 (Gaffney et al., 1998; Lee et al., 2012; Lee et al., 2008).

115 PAN was calibrated against standards synthesized by the nitration of peracetic acid in n-

116 tridecane (Gaffney et al., 1984; Gregory, 1990; Lee et al., 2008). A few microliter aliquots of

117 standard solution were injected through an injection valve and then mixed with zero air

118 (99.999 %) in a 5 L Tedlar bag. After being left for a few minutes for equilibrium, it was

injected into GC-luminol instrument and NOx chemiluminescence instrument with a molybdenum converter (42C, Thermo Electron Corporation, Franklin, MA, USA). The calibration was completed within 5 minutes to prevent thermal decomposition of the PAN (Kourtidis et al., 1993; Lee et al., 2008). These calibration procedures were carried out on the assumption that the PAN was completely converted to NO in the molybdenum converter. The detection limit of PAN defined by 3σ of the lowest standard was no greater than 100 pptv (Lee et al., 2008). The overall measurement uncertainty and precision was estimated to be 16 % and 5%, respectively (Lee et al., 2012). NO_x instrument was calibrated with NO standard gas.

Gaseous species including O_3, NO, NO_2, CO, and SO_2 were measured by UV absorption, chemiluminescence with a molybdenum converter, non-dispersive infrared, and pulse UV fluorescence method, respectively (NIER, 2016a). The measurements were made in compliance with guidelines for installation and operation of air pollution monitoring network (NIER, 2016b). Calibration was conducted before and after the experiment, following the regular checkup procedure. Detection limits of O_3, NO_x, CO, and SO_2 are 2 ppb, 0.1 ppb, 50 ppb, 0.1 ppb, respectively (NIER, 2016b).

Aerosol species, including $PM_{2.5}$ mass and $PM_{2.5}$ OC and EC were measured and recorded along with meteorological parameters (relative humidity, temperature, and wind direction and speed). Water-soluble ions of $PM_{1.0}$ were collected by a particle-into-liquid sampler (PILS) and analyzed by ion chromatography. The detailed results of the aerosol measurements can be found in Shang et al. (2017).

For the air parcel at 850 m a.s.l., the three-day backward trajectories were calculated every hour using NOAA Air Resources Laboratory (ARL) Hybrid Single-Particle Lagrangian Integrated Trajectory (HYSPLIT) model (version 4) (Draxler and Rolph, 2012; Rolph, 2012, http://www.arl.noaa.gov/ready/hysplit4.html). In addition, O_3 and PAN concentrations were

calculated using a global chemistry model, the Community Atmosphere Model with Chemistry (CAM-Chem), a component of the Community Earth System Model (CESM) (Lamarque et al., 2012; Tilmes et al., 2015). The CAM-chem results shown here follow the configuration used for the HTAP2 (Hemispheric Transport of Air Pollution, Phase 2) intercomparison (e.g., Stjern et al., 2016). CAM-chem is nudged to observed meteorology (GEOS-5) to reproduce the actual period of the observations (Oct 2010). The emissions used in the model are the HTAP2 inventory (Janssens-Maenhout, et al., 2015), which include the "MIX" Asian emissions inventory. Biomass burning emissions are from the Global Fire Emissions Database (GFED3) (Randerson et al., 2013).

3. Results

In the present experiments, PAN concentrations range from 0.1 to 2.4 ppbv, with an average of 0.6 ppbv. This mean value is lower than those observed in other Asian megacities: Beijing (1.41 ppb in the summer), Pearl River Delta region (1.32 ppb in the summer), and Seoul (0.8 ppb in the early summer); similar to those of suburban areas in China, e.g., Lanzhou (0.76 ppb in the summer); and higher than those of urban and rural sites in Japan, e.g., Tokyo (up to 0.6 ppb in the fall), Rishiri Island (~0.5 ppb in spring) or in the western coast of the US, e.g., Sacramento (0.45 ppb in the summer), Mt. Bachelor (0.144 ppb in the spring and early summer), off the western coast of the US (0.65 ppb in the spring), and over the remote North Pacific (total PAN < 0.3 ppb in spring) (Bertram et al., 2013; Fischer et al., 2011; La Franchi et al., 2009; Lee et al., 2008; Roberts et al., 2004; Tanimoto et al., 1999; Tanimoto et al., 2002; Wang et al., 2010; Zhang et al., 2009; Zhang et al., 2011). Because the PAN lifetime is greatly dependent on temperature, its concentration decreases with increasing

167 distance from the source regions. The PAN concentrations calculated in this study thus lie in-

168 between the levels for the East Asian megacities and the northern Pacific. The distributions of

169 all measured species, including PAN and O_3, are presented in Fig. 1. In particular, there are

170 several periods characterized by high concentrations of PAN, O_3, and $PM_{2.5}$. In terms of PAN,

171 four periods are particularly interesting (Fig. 1). High O_3 concentrations were observed

172 during October 31–November 2 [episode 1] but did not coincide with high PAN

173 concentrations. During October 28–29 [episode 2], NO_2 was noticeably increased. In

174 comparison, PAN and O_3 concentrations were both high during October 20–21 [episode 3]

175 and November 4–5 [episode 4]. Episodes 3 and 4 are characterized by haze, while episodes 1

176 and 2 are characterized by urban influence in the Korean and Beijing outflows, respectively.

177 Haze is reported by Korea Meteorological Administration (KMA) as a meteorological

178 phenomenon when visibility is 1~ 10 km and relative humidity is less than 75 %.

179   In the present study, PAN correlates reasonably well with O_3 ($\gamma = 0.67$) and even better

180 with $PM_{2.5}$ ($\gamma = 0.79$). In general, O_3 and PAN exhibit typical diurnal variation with a

181 maximum recorded in the afternoon, which results in a good correlation between the two

182 (Brasseur et al., 1999; Gaffney et al., 1999; Ridley et al., 1990; Schrimpf et al., 1995; Wang

183 et al., 2010). In this study, however, the O_3 peak was often found in the early morning and

184 late afternoon for several days (Fig. 1). Observing the diurnal variations in the entire PAN

185 concentration measurement set (Fig. 2), the maximum was clearly recorded in the morning

186 with the highest outliers, which is rather similar to that of $PM_{2.5}$. The diurnal pattern of NO_2

187 shows little variation, even though its concentrations were increased in the morning along

188 with PAN. This first measurement of PAN at GCO reveals that PAN is not always coupled

189 with O_3, which was not typically observed at remote sites in previous studies (e.g., Fischer et

190 al., 2010; Lee et al., 2012).

4.   Discussion

4.1.   Decoupling of PAN from O_3

To examine the detailed mechanism of the decoupling of PAN from O_3, the daily maximum concentrations of PAN and O_3 were further explored. The recorded daily PAN maxima were generally in good correlation with O_3, albeit the relationship did not seem to hold at high concentrations of PAN and O_3 (Fig. 3). The daily maxima were then categorized into four groups according to the time when each O_3 and PAN maximum was recorded: "O_3 day-PAN day", "O_3 day-PAN night", "O_3 night-PAN day", and "O_3 night-PAN night". The day interval started from 08:00 and ended at 18:00 (local time), based on the times of sunrise and sunset during the experiment period. While the high PAN concentrations were associated with the "O_3 day-PAN day" group (cross symbols in Fig. 3), the enhanced O_3 concentration was recorded in the "O_3 night-PAN night" group (star symbols in Fig. 3). The "O_3 night-PAN night" group unexpectedly held more data points than the "O_3 day-PAN day" group, even though the "O_3 night-PAN night" group concentrations were lower (Fig. 3). In addition, there were several days classified in the "O_3 night-PAN day" (marked by diamond) and "O_3 day-PAN night" groups, but with less frequency and lower concentrations. These results indicate that the decoupling of PAN from O_3 was primarily due the elevated concentrations of O_3 and PAN at night. While PAN reached the maximum during the day on Oct 20 and Nov 5, their concentrations were increased from the previous day through the night. The four high PAN and O_3 episodes identified in this study fall under the category of "O_3 night-PAN night" or "O_3 day-PAN day". These two cases will be further examined to identify the chemical and physical processes responsible for PAN being decoupled from O_3, instead of being coupled

215 with $PM_{2.5}$. The overall characteristics of the four episodes are summarized in Table 1.

216

4.2. Export of O_3 from Asian continents (episodes 1 & 2)

218

219   High O_3 concentrations were encountered around midnight on three consecutive days from

220 October 31 to November 2 (episode 1), during which SO_2 reached its maximum

221 concentration (Fig. 1). The backward trajectories of air masses revealed that air passed

222 through the Beijing area during this period (Fig. 4). The strong wind (13.5 m/s on average)

223 implies that it would take about a day for air mass leaving Beijing area to arrive at GCO.

224 The recorded O_3 maximum (80.6 ppbv) was concurrent with the PAN maximum (0.9 ppbv)

225 around midnight on November 1st (Fig. 1). All these results indicate that the air was heavily

226 influenced by outflow from the Beijing area, as previously hypothesized (Lim et al., 2012),

227 and that the nighttime enhancement of O_3 and PAN with SO_2 resulted from the fast transport

228 of urban plumes from China.

229   In previous studies, the nighttime enhancement of O_3 was observed at GCO (e.g., Lee et al.,

230 2007) in association with pollutant-laden air coming from Beijing. Similarly, Banta et al.

231 (1998) pointed out that the evening O_3 maximum was due to long-range transport of O_3 from

232 nearby urban areas. Wang et al. (2011) reported that the O_3 lifetime was about two days in

233 East China during the summer, which is sufficient for O_3 to travel to GCO but not for PAN

234 due to its short lifetime. Therefore, the nighttime maximum of O_3 can be attributed to the

235 export of O_3 from megacities in China, causing PAN to be decoupled from O_3. Because the

236 overall correlation between O_3 and PAN was the best with the highest $\Delta O_3/\Delta PAN$ among all

237 cases discussed in this study (Fig. 5a), episode 1 likely represents an event of rapid transport

238 from the Beijing area.

239   Another night maximum of O_3 was recorded on October 29. Note that NO_x was highly

elevated with the lowest SO_2 concentrations during October 28–29 (episode 2) (Fig. 1). In episode 2, O_3 concentrations were much lower and poorly correlated with those of PAN, compared to episode 1. Instead, PAN was best correlated with NO_2 with the highest $\Delta NO_2/\Delta PAN$ among all episodes (Fig. 5a, b). In this case, air masses passed through the Korean Peninsula, carrying low O_3 being titrated by high NO_x (Brasseur et al., 1999; Jacobson, 2005). These two episodes illustrate the export of urban plumes in northeast Asia region, which are distinguished by relative enhancement of reactive gases including O_3, PAN and NO_x, depending on the origin and aging of air masses.

4.3. PAN enhancement upon occurrence of haze (episodes 3 & 4)

In this study, two haze events were observed in the very beginning (October 20–21; episode 3) and the end of the study period (November 4–5; episode 4). As the nighttime O_3 peak was attributed to the transport from nearby urban areas to Jeju Island, the two haze episodes were also observed in association with continental outflows. The first haze event occurred on October 18th and lingered until October 21st, during which O_3 concentrations were gradually elevated. A second peak was recorded around midnight of October 19th and 20th, and the maximum was reached in the afternoon of October 20th (Figs. 1 and 3). In this episode, the maximum concentrations of O_3 and PAN were 78.9 ppbv and 2.0 ppbv, respectively, on October 20th, when the highest NO_2 concentration (12.7 ppbv) was observed under low wind speed (6.6 m/s daily average). The air mass trajectories suggest the influence of the Korean Peninsula, particularly the Seoul metropolitan area, in addition to East China (Fig. 4).

In the second haze event (episode 4), an air mass was slowly transported from East China,

264 including the Jiangsu province, under stagnant condition which was developed by an

265 anticyclone system (Fig. 4). We measured the highest concentrations of all aerosol species

266 including the PM$_{2.5}$ mass as well as PAN and O$_3$, which were 156 μg/m^3, 2.4 ppbv, and 87.5

267 ppbv, respectively. Other reactive gases such as CO, SO$_2$, and NO$_2$ were also highly elevated.

268 Note that PAN and O$_3$ gradually increased through the night, leading to a nighttime maximum

269 of both species on November 4th. It is likely that the pre-formed PAN and O$_3$ were

270 continuously transported into Gosan at night.

271   PAN is formed through the reaction of the peroxyacetyl radical and nitrogen dioxide (Eq. 1)

272 and decomposed at high temperature (Eq. 2), returning these radicals. Unless the NO

273 concentration is high (Eq. 3), the peroxyacetyl radical recombines with NO$_2$, producing PAN.

274 Thus, the total lifetime of PAN depends on the NO$_2$/NO ratio and temperature (Eq. 4)

275 (Brasseur et al., 1999).

276 $$CH_3C(O)O_2 + NO_2 + M \rightarrow PAN + M \quad (1)$$

277 $$PAN \rightarrow CH_3C(O)O_2 + NO_2 \quad\quad (2)$$

278 $$CH_3C(O)O_2 + NO \rightarrow CH_3CO_2 + NO_2 \quad (3)$$
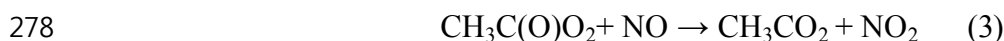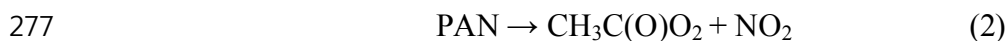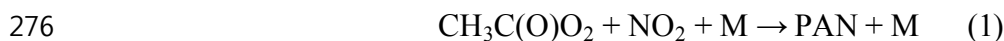
279 $$T_{eff} = T_d \left(1 + \frac{k_1[NO_2]}{k_2[NO]} \right) \ [\text{sec}^{-1}] \quad\quad (4)$$

280 where T_d and T_{eff} indicate the lifetime against decomposition and the effective lifetime of

281 PAN (Brasseur et al., 1999). The effective lifetime of PAN was estimated through Eq. 4 using

282 the rate constants proposed by Brasseur et al. (1999), Jacobson (2005), and Maricq and

283 Szente (1996).

284   During the haze event, NO was close to the detection limit, while NO$_2$ was greatly

285 enhanced. Owing to the high NO$_2$/NO ratio, the effective lifetime of PAN increased by 57

286 times; this possibly contributed to the gradual increase in PAN through the night on

287 November 4th. Fischer et al. (2014) also reported that, at night, PAN can be produced from

288 the reaction of acetaldehyde with the nitrate radical.

289   Besides PM$_{2.5}$ mass, PAN was also well correlated with PM$_{2.5}$ OC and EC not only during

290   this haze episode but also during the entire measurement period (Fig. 6a and b). Furthermore,

291   the enhancement of PAN was concurrent with that of OC and K$^+$, resulting in excellent

292   correlation between them (Fig. 6b and d). In fact, the ΔOC/ΔEC ratio of episode 4 was much

293   higher (7) than those of the other episodes (~2.5) (Fig. 6c). The fraction of PM$_{2.5}$ against

294   PM$_{10}$ was also the highest in this episode, indicating significant contribution of secondary

295   aerosols. These observations suggest that air masses were affected by biomass combustion

296   (e.g., Ram et al., 2008, 2012; Saarikoski et al., 2008).

297   According to previous studies, PAN can be produced in plumes through biomass

298   combustion (Alvarado et al., 2010; Coheur et al., 2007; Liu et al., 2016b; Tereszchuk et al.,

299   2013). In northeast China, open burnings related to agricultural activities frequently occur

300   during the spring and fall (Duan et al., 2004; Yang et al., 2005). Kudo et al. (2014) also

301   reported that, upon burning crop residue in Yangtze region, the levels of oxygenated VOCs

302   were elevated together with NO$_x$. In addition, biofuel is used for cooking and heating and as

303   an energy source in China's industry (Cao et al., 2006).

304   Therefore, PAN is likely to increase when haze occurs and fine aerosols are transformed as

305   air masses carrying combustion emissions are slowly transported from China over the Yellow

306   Sea. Additionally, the results of this study imply that PAN can be used as a robust tracer for

307   continental outflows in northeast Asia, to identify transport- and chemical transformation-

308   dominant regimes. In a transport-dominant regime, O$_3$ export was distinguished by the

309   highest levels of primary gaseous species such as SO$_2$ and relatively low levels of PAN. In

310   contrast, fine aerosol species were enhanced in a chemical transformation regime, leading to

311   haze events with relatively more enhanced PAN compared to O$_3$.

312   Finally, the measured O$_3$ and PAN concentrations were compared to results from a global

313   chemistry model CAM-Chem. In the model simulation, O_3 and PAN were highly

314   underestimated during the episodes observed in Chinese outflows, although the variation

315   around average level of O_3 and PAN was well captured (Fig. 7). The elevated PAN

316   concentration was underestimated in the model (Oct 20–21 and Nov 4–5), especially when air

317   was impacted by biomass combustion. The timing of the O_3 diurnal variability was captured

318   by the model, although the magnitude of the variation was underestimated. These results

319   reveal that the current understanding of Chinese outflow is still not sufficient, thereby causing

320   uncertainty in estimating its effect on air quality in the northwestern Pacific Rim.

321

322   **5.   Conclusions**

323

324   The first measurements of PAN, reactive gases, and aerosol species were conducted at

325   GCO during October 19 to November 6, 2010. The average concentration of PAN was 0.6

326   ppbv with a maximum of 2.4 ppbv, which was lower than those in major cities in East Asia

327   but much higher than the background concentrations in other regions. Although the hourly

328   concentrations of PAN and O_3 were well correlated ($\gamma = 0.67$), the comparison of the daily

329   maxima of PAN and O_3 highlighted that they were not proportionally enhanced. That is,

330   either PAN was relatively more elevated than O_3 or the highest O_3 was associated with low

331   levels of PAN. Unexpectedly, both PAN and O_3 often reached their maxima at night. In this

332   study, these high concentrations were all encountered in association with continental outflows,

333   where PAN was decoupled from O_3 and better correlated with the $PM_{2.5}$ mass ($\gamma = 0.79$) than

334   with O_3. Thus, two high-O_3 and two high-PAN events were the most clearly distinguished

335   and investigated in detail.

336   During the O_3 episodes, both O_3 and PAN concentrations reached their maximum values at

337 night. In episode 1 (Oct. 31 to Nov. 2), the O_3 concentration was increased to 80.6 ppbv, with

338 a high SO_2 concentration under strong wind. It was a typical Beijing plume observed in the

339 study region. In comparison, NO_2 was greatly increased in episode 2 (Oct. 28–29) when the

340 air masses were affected by urban emissions from Korean Peninsula. Although the maximum

341 O_3 level was lower during episode 2, these two cases demonstrated well how O_3 was exported

342 from the East Asian continent.

343 The remaining two episodes were highlighted by enhanced PAN concentrations and

344 characterized by haze occurrence. During episode 3 (Oct. 20–21), PAN and O_3 concentrations

345 increased up to 2.0 ppbv and 78.9 ppbv, respectively, with high NOx levels, probably

346 influenced by emissions from Korea. Episode 4 (Nov. 4–5) was characterized by the highest

347 concentrations of almost all measured species, including PAN, O_3, $PM_{2.5}$ mass, and $PM_{1.0}$

348 species; the maximum recorded concentrations of PAN, O_3, and $PM_{2.5}$ mass during this

349 interval were 2.4 ppbv, 87.5 ppbv, and 156 $\mu g/m^3$, respectively. Note that, along with $PM_{2.5}$

350 and O_3, PAN was gradually increased through the night. In this episode, an air mass was

351 slowly transported from eastern China. With depleted NO, the effective lifetime of PAN was

352 greatly extended. In addition, PAN concentration showed good correlation with OC, EC, and

353 K^+; in fact, the correlation of PAN with K^+ was comparable to that of OC with K^+. These

354 results, in conjunction with the high OC/EC (7), imply that the observed haze was mainly

355 caused by the emissions produced by biomass combustion. These results suggest that PAN is

356 a useful tool for distinguishing continental outflows that were typically observed in northeast

357 Asia.

358 The comparison between the measured and calculated concentrations using the CAM-

359 Chem-HTAP2 model showed that the model underestimated the O_3 and PAN levels in

360 Chinese outflows, particularly for haze incidence. These results reveal that Chinese outflows

361   are still poorly understood and not well captured in the model.

362

363   **Acknowledgments**

364   This study was funded by the Korea Meteorological Administration Research and

365   Development Program under Grant KMIPA 2015-6020. The National Center for Atmospheric

366   Research is funded by the National Science Foundation. The authors gratefully acknowledge

367   the NOAA Air Resources Laboratory (ARL) for the provision of the HYSPLIT transport and

368   dispersion model and/or READY website (http://www.ready.noaa.gov) used in this

369   publication.

References

Akimoto, H.: Global air quality and pollution, Science, 302, 1716-1719, doi:10.1126/science.1092666, 2003.

Alvarado, M. J., Logan, J. A., Mao, J., Apel, E., Riemer, D., Blake, D., Cohen, R. C., Min, K. E., Perring, A. E., Browne, E. C., Wooldridge, P. J., Diskin, G. S., Sachse, G. W., Fuelberg, H., Sessions, W. R., Harrigan, D. L., Huey, G., Liao, J., Case-Hanks, A., Jimenez, J. L., Cubison, M. J., Vay, S. A., Weinheimer, A. J., Knapp, D. J., Montzka, D. D., Flocke, F. M., Pollack, I. B., Wennberg, P. O., Kurten, A., Crounse, J., Clair, J. M. S., Wisthaler, A., Mikoviny, T., Yantosca, R. M., Carouge, C. C., and Le Sager, P.: Nitrogen oxides and PAN in plumes from boreal fires during ARCTAS-B and their impact on ozone: an integrated analysis of aircraft and satellite observations, Atmos. Chem. Phys., 10, 9739-9760, doi:10.5194/acp-10-9739-2010, 2010.

Aneja, V. P., Hartsell, B. E., Kim, D. S., and Grosjean, D.: Peroxyacetyl nitrate in Atlanta, Georgia: Comparison and analysis of ambient data for suburban and downtown locations, J. Air & Waste Manage. Assoc., 49, doi: 177-184, 10.1080/10473289.1999.10463786, 1999.

Banta, R. M., Senff, C. J., White, A. B., Trainer, M., McNider, R. T., Valente, R. J., Mayor, S. D., Alvarez, R. J., Hardesty, R. M., Parrish, D., and Fehsenfeld, F. C.: Daytime buildup and nighttime transport of urban ozone in the boundary layer during a stagnation episode, J. Geophys. Res. Atmos., 103, 22519-22544, doi:10.1029/98jd01020, 1998.

Beine, H. J., Jaffe, D. A., Herring, J. A., Kelley, J. A., Krognes, T., and Stordal, F.: High-latitude springtime photochemistry .1. NOx, PAN and ozone relationships, J. Atmos. Chem., 27, 127-153, doi:10.1023/a:1005869900567, 1997.

Bertram, T. H., Perring, A. E., Wooldridge, P. J., Dibb, J., Avery, M. A., and Cohen, R. C.: On the export of reactive nitrogen from Asia: NO_x partitioning and effects on ozone, Atmos. Chem. Phys., 13, 4617-4630, doi:10.5194/acp-13-4617-2013, 2013.

Brasseur, G. P., Orlando, J. J., and Tyndall, G. S.: Atmospheric chemistry and global change, Oxford University Press, New York, 235-347 pp., 1999.

Cao, G., Zhang, X., and Zheng, F.: Inventory of black carbon and organic carbon emissions from China, Atmos. Environ., 40, 6516-6527, doi:10.1016/j.atmosenv.2006.05.070, 2006.

Coheur, P. F., Herbin, H., Clerbaux, C., Hurtmans, D., Wespes, C., Carleer, M., Turquety, S., Rinsland, C. P., Remedios, J., Hauglustaine, D., Boone, C. D., and Bernath, P. F.: ACE-FTS observation of a young biomass burning plume: first reported measurements of C_2H_4, C_3H_6O, H_2CO and PAN by infrared occultation from space, Atmos. Chem. Phys., 7, 5437-5446, doi:10.5194/acp-7-5437-2007, 2007.

Draxler, R. R., and Rolph, G. D.: HYSPLIT (HYbrid Single-Particle Lagrangian Integrated Trajectory) Model access via NOAA ARL READY Website (http://ready.arl.noaa.gov/HYSPLIT.php), NOAA Air Resources Laboratory, Silver Spring, MD., 2012.

Duan, F., Liu, X., Yu, T., and Cachier, H.: Identification and estimate of biomass burning contribution to the urban aerosol organic carbon concentrations in Beijing, Atmos. Environ., 38, 1275-1282, doi:10.1016/j.atmosenv.2003.11.037, 2004.

Fischer, E. V., Jaffe, D. A., Reidmiller, D. R., and Jaeglé, L.: Meteorological controls on observed peroxyacetyl nitrate at Mount Bachelor during the spring of 2008, J. Geophys. Res., 115, D03302, doi:10.1029/2009jd012776, 2010.

Fischer, E. V., Jaffe, D. A., and Weatherhead, E. C.: Free tropospheric peroxyacetyl nitrate (PAN) and ozone at Mount Bachelor: potential causes of variability and timescale for trend detection, Atmos. Chem. Phys., 11, 5641-5654, doi:10.5194/acp-11-5641-2011, 2011.

Fischer, E. V., Jacob, D. J., Yantosca, R. M., Sulprizio, M. P., Millet, D. B., Mao, J., Paulot, F., Singh, H. B., Roiger, A., Ries, L., Talbot, R. W., Dzepina, K., and Pandey, D. S.: Atmospheric peroxyacetyl nitrate (PAN): a global budget and source attribution, Atmos. Chem. Phys., 14, 2679-2698, doi:10.5194/acp-14-2679-2014, 2014.

Gaffney, J. S., Fajer, R., and Senum, G. I.: An improved procedure for high purity gaseous peroxyacyl nitrate production: Use of heavy lipid solvents, Atmos. Environ., 18, 215-218, doi:10.1016/0004-6981(84)90245-2, 1984.

Gaffney, J. S., Bornick, R. M., Chen, Y. H., and Marley, N. A.: Capillary gas chromatographic analysis of nitrogen dioxide and pans with luminol chemiluminescent detection, Atmos. Environ., 32, 1445-1454, doi:10.1016/S1352-2310(97)00098-8, 1998.

Gaffney, J. S., Marley, N. A., Cunningham, M. M., and Doskey, P. V.: Measurements of peroxyacyl nitrates (PANs) in Mexico City: implications for megacity air quality impacts on regional scales, Atmos. Environ., 33, 5003-5012, doi:10.1016/S1352-2310(99)00263-0, 1999.

Gallagher, M. S., Carsey, T. P., and Farmer, M. L.: Peroxyacetyl nitrate in the North Atlantic marine boundary layer, Global Biogeochem. Cycle., 4, 297-308, doi:10.1029/GB004i003p00297, 1990.

Gregory, G. L.: An intercomparison of airborne PAN measurements, J. Geophys. Res., 95, 10077-10087, doi:10.1029/JD095iD07p10077, 1990.

Grosjean, E., Grosjean, D., Woodhouse, L. F., and Yang, Y.-J.: Peroxyacetyl nitrate and peroxypropionyl nitrate in Porto Alegre, Brazil, Atmos. Environ., 36, 2405-2419, doi:10.1016/S1352-2310(01)00541-6, 2002.

Gu, D., Wang, Y., Smeltzer, C., and Liu, Z.: Reduction in NOx Emission Trends over China: Regional and Seasonal Variations, Environ. Sci. Technol., 47, 12912–12919, doi:10.1021/es401727e, 2013.

Hansel, A., and Wisthaler, A.: A method for real-time detection of PAN, PPN and MPAN in ambient air, Geophys. Res. Lett., 27, 895-898, doi:10.1029/1999gl010989, 2000.

Jacob, D. J.: Introduction to atmospheric chemistry, 199-231 pp., 1999.

Jacob, D. J.: Heterogeneous chemistry and tropospheric ozone, Atmos. Environ., 34, 2131-2159, doi:10.1016/s1352-2310(99)00462-8, 2000.

Jacobson, M. Z.: Fundamentals of atmospheric modeling, Second edition, Cambridge, UK, 731-738 pp., 2005.

Jaffe, D. A., Thornton, J., Wolfe, G., Reidmiller, D., Fischer, E. V., Jacob, D. J., Zhang, L., Cohen, R., Singh, H., Weinheimer, A., and Flocke, F.: Can we detect an Influence over North America from Increasing Asian NOx Emissions?, Eos Trans, AGU, 88, 2007.

Janssens-Maenhout, G., Crippa, M., Guizzardi, D., Dentener, F., Muntean, M., Pouliot, G., Keating, T., Zhang, Q., Kurokawa, J., Wankmüller, R., Denier van der Gon, H., Kuenen, J. J. P., Klimont, Z., Frost, G., Darras, S., Koffi, B., and Li, M.: HTAP_v2.2: a mosaic of regional and global emission grid maps for 2008 and 2010 to study hemispheric transport of air pollution, Atmos. Chem. Phys., 15, 11411-11432, doi:10.5194/acp-15-11411-2015, 2015.

Kanaya, Y., Tanimoto, H., Matsumoto, J., Furutani, H., Hashimoto, S., Komazaki, Y., Tanaka, S., Yokouchi, Y., Kato, S., Kajii, Y., and Akimoto, H.: Diurnal variations in H_2O_2, O_3, PAN, HNO_3 and aldehyde concentrations and NO/NO_2 ratios at Rishiri Island, Japan: Potential influence from iodine chemistry, Sci. Total Envir., 376, 185-197, doi:10.1016/j.scitotenv.2007.01.073, 2007.

Kenley, R. A., and Hendry, D. G.: Generation of peroxy radicals from peroxynitrates ($ROONO_2$). Decomposition of peroxybenzoyl nitrate (PBzN), J. Am. Chem. Soc., 104, 220-224, doi:10.1021/ja00365a040, 1982.

Kourtidis, K. A., Fabian, P., Zerefos, C., and RappenglÜCk, B.: Peroxyacetyl nitrate (PAN), peroxypropionyl nitrate (PPN) and PAN/ozone ratio measurements at three sites in Germany, Tellus B, 45, 442-457, doi:10.1034/j.1600-0889.1993.t01-3-00004.x, 1993.

Krotkov, N. A., McLinden, C. A., Li, C., Lamsal, L. N., Celarier, E. A., Marchenko, S. V., Swartz, W. H., Bucsela, E. J., Joiner, J., Duncan, B. N., Boersma, K. F., Veefkind, J. P., Levelt, P. F., Fioletov, V. E., Dickerson, R. R., He, H., Lu, Z., and Streets, D. G.: Aura OMI observations of regional SO2 and NO2 pollution changes from 2005 to 2015, Atmos. Chem. Phys., 16, 4605–4629, doi:10.5194/acp-16-4605-2016, 2016.

Kudo, S., Tanimoto, H., Inomata, S., Saito, S., Pan, X., Kanaya, Y., Taketani, F., Wang, Z., Chen, H., Dong, H., Zhang, M., and Yamaji, K.: Emissions of nonmethane volatile organic compounds from open crop residue burning in the Yangtze River Delta region, China, J. Geophys. Res., 119, 7684–7698, doi:10.1002/2013JD021044, 2014.

LaFranchi, B. W., Wolfe, G. M., Thornton, J. A., Harrold, S. A., Browne, E. C., Min, K. E., Wooldridge, P. J., Gilman, J. B., Kuster, W. C., Goldan, P. D., De Gouw, J. A., McKay, M., Goldstein, A. H., Ren, X., Mao, J., and Cohen, R. C.: Closing the peroxy acetyl nitrate budget: Observations of acyl peroxy nitrates (PAN, PPN, and MPAN) during BEARPEX 2007, Atmos. Chem. Phys., 9, 7623-7641, doi:10.5194/acp-9-7623-2009, 2009.

Lamarque, J. F., Emmons, L. K., Hess, P. G., Kinnison, D. E., Tilmes, S., Vitt, F., Heald, C. L., Holland, E. A., Lauritzen, P. H., Neu, J., Orlando, J. J., Rasch, P. J., and Tyndall, G. K.: CAM-chem: description and evaluation of interactive atmospheric chemistry in the Community Earth System Model, Geosci. Model Dev., 5, 369-411, doi:10.5194/gmd-5-369-2012, 2012.

Lee, G., Jang, Y., Lee, H., Han, J.-S., Kim, K.-R., and Lee, M.: Characteristic behavior of peroxyacetyl nitrate (PAN) in Seoul megacity, Korea, Chemosphere, 73, 619-628, doi:10.1016/j.chemosphere.2008.05.060, 2008.

Lee, G., Choi, H.-S., Lee, T., Choi, J., Park, J. S., and Ahn, J. Y.: Variations of regional background peroxyacetyl nitrate in marine boundary layer over Baengyeong Island, South Korea, Atmos. Environ., 61, 533-541, doi:10.1016/j.atmosenv.2012.07.075, 2012.

Lee, M., Song, M., Moon, K. J., Han, J. S., Lee, G., and Kim, K.-R.: Origins and chemical

characteristics of fine aerosols during the northeastern Asia regional experiment (Atmospheric Brown Cloud-East Asia Regional Experiment 2005), J. Geophys. Res., 112, D22S29, doi:10.1029/2006jd008210, 2007.

Li, M., Zhang, Q., Kurokawa, J., Woo, J. H., He, K. B., Lu, Z., Ohara, T., Song, Y., Streets, D. G., Carmichael, G. R., Cheng, Y. F., Hong, C. P., Huo, H., Jiang, X. J., Kang, S. C., Liu, F., Su, H., and Zheng, B.: MIX: a mosaic Asian anthropogenic emission inventory for the MICS-Asia and the HTAP projects, Atmos. Chem. Phys. Discuss., 2015, 34813-34869, doi:10.5194/acpd-15-34813-2015, 2015.

Lim, S., Lee, M., Lee, G., Kim, S., Yoon, S., and Kang, K.: Ionic and carbonaceous compositions of PM_{10}, $PM_{2.5}$ and $PM_{1.0}$ at Gosan ABC Superstation and their ratios as source signature, Atmos. Chem. Phys., 12, 2007-2024, doi:10.5194/acp-12-2007-2012, 2012.

Liu, F., Zhang, Q., A., van der A, R. J., Zheng, B., Tong, D., Yan, L., Zheng, Y., and He, K.: Recent reduction in NO x emissions over China: synthesis of satellite observations and emission inventories, Environmental Research Letters, 11, 114002, doi:10.1088/1748-9326/11/11/114002, 2016a.

Liu, Z., Wang, Y., Gu, D., Zhao, C., Huey, L. G., Stickel, R., Liao, J., Shao, M., Zhu, T., Zeng, L., Liu, S.-C., Chang, C.-C., Amoroso, A., and Costabile, F.: Evidence of reactive aromatics as a major source of peroxy acetyl nitrate over China, Environ. Sci. Technol., 44, 7017-7022, doi:10.1021/es1007966, 2010.

Liu, X., Zhang, Y., Huey, L. G., Yokelson, R. J., Wang, Y., Jimenez, J. L., Campuzano-Jost, P., Beyersdorf, A. J., Blake, D. R., Choi, Y., St. Clair, J. M., Crounse, J. D., Day, D. A., Diskin, G. S., Fried, A., Hall, S. R., Hanisco, T. F., King, L. E., Meinardi, S., Mikoviny, T., Palm, B. B., Peischl, J., Perring, A. E., Pollack, I. B., Ryerson, T. B., Sachse, G., Schwarz, J. P., Simpson, I. J., Tanner, D. J., Thornhill, K. L., Ullmann, K., Weber, R. J., Wennberg, P. O., Wisthaler, A., Wolfe, G. M., and Ziemba, L. D.: Agricultural fires in the southeastern U.S. during SEAC4RS: Emissions of trace gases and particles and evolution of ozone, reactive nitrogen, and organic aerosol, J. Geophys, Res.- Atmos., 121, 7383-7414, doi:10.1002/2016JD025040, 2016b.

Maricq, M. M., and Szente, J. J.: Temperature-dependent study of the $CH_3C(O)O_2$ + NO reaction, J. Phys. Chem., 100, 12380-12385, doi:10.1021/jp960792c, 1996.

Marley, N. A., Gaffney, J. S., White, R. V., Rodriguez-Cuadra, L., Herndon, S. E., Dunlea, E., Volkamer, R. M., Molina, L. T., and Molina, M. J.: Fast gas chromatography with luminol chemiluminescence detection for the simultaneous determination of nitrogen dioxide and peroxyacetyl nitrate in the atmosphere, Rev. Sci. Instr., 75, 4595-4605, doi:10.1063/1.1805271, 2004.

Mills, G. P., Sturges, W. T., Salmon, R. A., Bauguitte, S. J. B., Read, K. A., and Bandy, B. J.: Seasonal variation of peroxyacetylnitrate (PAN) in coastal Antarctica measured with a new instrument for the detection of sub-part per trillion mixing ratios of PAN, Atmos. Chem. Phys., 7, 4589-4599, doi:10.5194/acp-7-4589-2007, 2007.

Muller, K. P., and Rudolph, J.: Measurements of peroxyacetylnitrate in the marine boundary layer over the Atlantic, J. Atmos. Chem., 15, 361-367, doi:10.1007/BF00115405, 1992.

Nielsen, T., Samuelsson, U., Grennfelt, P., and Thomsen, E. L.: Peroxyacetyl nitrate in long-range transported polluted air, Nature, 293, 553-555, doi:10.1038/293553a0, 1981.

NIER, Annual Report of Ambient Air Quality in Korea, 2015, National Institute of Environmental Research, Inchon, Korea, 350pp., 2016a (in Korean).

NIER, Guidelines for installation and operation of air pollution monitoring network, National Institute of Environmental Research, Inchon, Korea, 427 pp., 2016b (in Korean).

Ohara, T., Akimoto, H., Kurokawa, J., Horii, N., Yamaji, K., Yan, X., and Hayasaka, T.: An Asian emission inventory of anthropogenic emission sources for the period 1980-2020, Atmos. Chem. Phys., 7, 4419-4444, doi:10.5194/acp-7-4419-2007, 2007.

Ram, K., Sarin, M. M., and Hegde, P.: Atmospheric abundances of primary and secondary carbonaceous species at two high-altitude sites in India: Sources and temporal variability, Atmos. Environ., 42, 6785-6796, doi:10.1016/j.atmosenv.2008.05.031, 2008.

Ram, K., Sarin, M. M., and Tripathi, S. N.: Temporal trends in atmospheric $PM_{2.5}$, PM_{10}, elemental carbon, organic carbon, water-soluble organic carbon, and optical properties: Impact of biomass burning emissions in the Indo-Gangetic Plain, Environ. Sci. Technol., 46, 686-695, doi:10.1021/es202857w, 2012.

Randerson, J. T., van der Werf, G. R., Giglio, L., Collatz, G. J., and Kasibhatla, P. S.: Global Fire Emissions Database, Version 3 (GFEDv3.1). Data set. Available on-line [http://daac.ornl.gov/] from Oak Ridge National Laboratory Distributed Active Archive Center, Oak Ridge, Tennessee, USA. doi:10.3334/ORNLDAAC/1191, 2013.

Ridley, B. A., Shetter, J. D., Gandrud, B. W., Salas, L. J., Singh, H. B., Carroll, M. A., Hubler, G., Albritton, D. L., Hastie, D. R., Schiff, H. I., Mackay, G. I., Karechi, D. R., Davis, D. D., Bradshaw, J. D., Rodgers, M. O., Sandholm, S. T., Torres, A. L., Condon, E. P., Gregory, G. L., and Beck, S. M.: Ratios of peroxyacetyl nitrate to active nitrogen observed during aircraft flights over the Eastern Pacific Oceans and continental United-States, J. Geophys. Res., 95, 10179-10192, doi:10.1029/JD095iD07p10179, 1990.

Roberts, J. M., Flocke, F., Chen, G., de Gouw, J., Holloway, J. S., Hübler, G., Neuman, J. A., Nicks, D. K., Nowak, J. B., Parrish, D. D., Ryerson, T. B., Sueper, D. T., Warneke, C., and Fehsenfeld, F. C.: Measurement of peroxycarboxylic nitric anhydrides (PANs) during the ITCT 2K2 aircraft intensive experiment, J. Geophys, Res.- Atmos., 109, D23S21, doi:10.1029/2004JD004960, 2004.

Roberts, J. M., Marchewka, M., Bertman, S. B., Sommariva, R., Warneke, C., de Gouw, J., Kuster, W., Goldan, P., Williams, E., Lerner, B. M., Murphy, P., and Fehsenfeld, F. C.: Measurements of PANs during the New England Air Quality Study 2002, J. Geophys. Res., 112, D20306, doi:10.1029/2007JD008667, 2007.

Rolph, G. D.: Real-time Environmental Applications and Display sYstem (READY) Website (http://ready.arl.noaa.gov). NOAA Air Resources Laboratory, Silver Spring, MD. , 2012.

Saarikoski, S., Timonen, H., Saarnio, K., Aurela, M., Jrvi, L., Keronen, P., Kerminen, V. M., and Hillamo, R.: Sources of organic carbon in fine particulate matter in northern European urban air, Atmos. Chem. Phys., 8, 6281-6295, doi:10.5194/acp-8-6281-2008, 2008.

Schrimpf, W., Muller, K. P., Johnen, F. J., Lienaerts, K., and Rudolph, J.: An optimized method for airborne peroxyacetyl nitrate (PAN) measurements, J. Atmos. Chem., 22, 303-317, doi:10.1007/bf00696640, 1995.

Shang, X., Lee, M., Han, J., Kang, E., Gustafsson, Ö., and Chang, L.-S.: Identifiction and

chemical characteristics of distinctive Chinese outflow plumes associated with enhanced submicron aerosols at Gosan Climate Observatory, submitted at Aerosol Air Qual. Res.

Staudt, A. C., Jacob, D. J., Ravetta, F., Logan, J. A., Bachiochi, D., Sandholm, S., Ridley, B., Singh, H. B., and Talbot, B.: Sources and chemistry of nitrogen oxides over the tropical Pacific, J. Geophys. Res., 108, 8239, doi:10.1029/2002JD002139, 2003.

Stjern, C. W., Samset, B. H., Myhre, G., Bian, H., Chin, M., Davila, Y., Dentener, F., Emmons, L., Flemming, J., Haslerud, A. S., Henze, D., Jonson, J. E., Kucsera, T., Lund, M. T., Schulz, M., Sudo, K., Takemura, T., and Tilmes, S.: Global and regional radiative forcing from 20% reductions in BC, O C and SO4 – an HTAP2 multi-model study, Atmos. Chem. Phys., 16, 13579-13599, doi:10.5194/acp-16-13579-2016, 2016.

Talukdar, R. K., Burkholder, J. B., Schmoltner, A. M., Roberts, J. M., Wilson, R. R., and Ravishankara, A. R.: Investigation of the loss processes for peroxyacetyl nitrate in the atmosphere: UV photolysis and reaction with OH, J. Geophys. Res., 100, 14163-14173, doi:10.1029/95JD00545, 1995.

Tanimoto, H., Hirokawa, J., Kajii, Y., and Akimoto, H.: A new measurement technique of peroxyacetyl nitrate at parts per trillion by volume levels: Gas chromatography/negative ion chemical ionization mass spectrometry, J. Geophys. Res., 104(17), 21, 343-21, 354, doi:10.1029/1999JD900345, 1999.

Tanimoto, H., H. Furutani, S. Kato, J. Matsumoto, Y. Makide, and H. Akimoto, Seasonal cycles of ozone and oxidized nitrogen species in northeast Asia, 1, Impact of regional climatology and photochemistry observed during RISOTTO 1999-2000, J. Geophys. Res., 107(D24), 4747, doi:10.1029/2001JD001496, 2002.

Tanimoto, H., K. Matsumoto, and M. Uematsu, Ozone−CO correlations in Siberian wildfire plumes observed at Rishiri Island, SOLA, 4, 65-68, doi:10.2151/sola.2008-017, 2008.

Tereszchuk, K. A., Moore, D. P., Harrison, J. J., Boone, C. D., Park, M., Remedios, J. J., Randel, W. J., and Bernath, P. F.: Observations of peroxyacetyl nitrate (PAN) in the upper troposphere by the Atmospheric Chemistry Experiment-Fourier Transform Spectrometer (ACE-FTS), Atmos. Chem. Phys., 13, 5601-5613, doi:10.5194/acp-13-5601-2013, 2013.

Tilmes, S., Lamarque, J. F., Emmons, L. K., Kinnison, D. E., Ma, P. L., Liu, X., Ghan, S., Bardeen, C., Arnold, S., Deeter, M., Vitt, F., Ryerson, T., Elkins, J. W., Moore, F., Spackman, J. R., and Val Martin, M.: Description and evaluation of tropospheric chemistry and aerosols in the Community Earth System Model (CESM1.2), Geosci. Model Dev., 8, 1395-1426, doi:10.5194/gmd-8-1395-2015, 2015.

Villena, G., Bejan, I., Kurtenbach, R., Wiesen, P., and Kleffmann, J.: Interferences of commercial NO2 instruments in the urban atmosphere and in a smog chamber, Atmos. Meas. Tech., 5, 149-159, dio:10.5194/amt-5-149-2012, 2012.

Wang, B., Shao, M., Roberts, J. M., Yang, G., Yang, F., Hu, M., Zeng, L., Zhang, Y., and Zhang, J.: Ground-based on-line measurements of peroxyacetyl nitrate (PAN) and peroxypropionyl nitrate (PPN) in the Pearl River Delta, China, Int. J. Environ. Anal. Chem., 90, 548-559, doi:10.1080/03067310903194972, 2010.

Wang, Y., Zhang, Y., Hao, J., and Luo, M.: Seasonal and spatial variability of surface ozone over China: contributions from background and domestic pollution, Atmos. Chem. Phys.,

629   11, 3511-3525, doi:10.5194/acp-11-3511-2011, 2011.

Yang, F., He, K., Ye, B., Chen, X., Cha, L., Cadle, S. H., Chan, T., and Mulawa, P. A.: One-year record of organic and elemental carbon in fine particles in downtown Beijing and Shanghai, Atmos. Chem. Phys., 5, 1449-1457, doi:10.5194/acp-5-1449-2005, 2005.

Zhang, H., Xu, X., Lin, W., and Wang, Y.: Wintertime peroxyacetyl nitrate (PAN) in the megacity Beijing: Role of photochemical and meteorological processes, J. Environ. Sci., 26, 83-96, doi:10.1016/S1001-0742(13)60384-8, 2014.

Zhang, J. B., Xu, Z., Yang, G., and Wang, B.: Peroxyacetyl nitrate (PAN) and peroxypropionyl nitrate (PPN) in urban and suburban atmospheres of Beijing, China, Atmos. Chem. Phys. Discuss., 11, 8173-8206, doi:10.5194/acpd-11-8173-2011, 2011.

Zhang, J. M., Wang, T., Ding, A. J., Zhou, X. H., Xue, L. K., Poon, C. N., Wu, W. S., Gao, J., Zuo, H. C., Chen, J. M., Zhang, X. C., and Fan, S. J.: Continuous measurement of peroxyacetyl nitrate (PAN) in suburban and remote areas of western China, Atmos. Environ., 43, 228-237, doi:10.1016/j.atmosenv.2008.09.070, 2009.

Zhang, L., Jacob, D. J., Boersma, K. F., Jaffe, D. A., Olson, J. R., Bowman, K. W., Worden, J. R., Thompson, A. M., Avery, M. A., Cohen, R. C., Dibb, J. E., Flock, F. M., Fuelberg, H. E., Huey, L. G., McMillan, W. W., Singh, H. B., and Weinheimer, A. J.: Transpacific transport of ozone pollution and the effect of recent Asian emission increases on air quality in North America: An integrated analysis using satellite, aircraft, ozonesonde, and surface observations, Atmos. Chem. Phys., 8, 6117-6136, doi:10.5194/acp-8-6117-2008, 2008.

Zhao, B., Wang, S. X., Liu, H., Xu, J. Y., Fu, K., Klimont, Z., Hao, J. M., He, K. B., Cofala, J., and Amann, M.: NOx emissions in China: historical trends and future perspectives, Atmos. Chem. Phys., 13, 9869–9897, doi:10.5194/acp-13-9869-2013, 2013.

Zhu, L., Fischer, E. V., Payne, V. H., Worden, J. R., and Jiang, Z.: TES observations of the interannual variability of PAN over Northern Eurasia and the relationship to springtime fires, Geophys. Res. Lett., 42, 7230-7237, dio:10.1002/2015GL065328, 2015.

Zhu, L., Payne, V. H., Walker, T. W., Worden, J. R., Jiang, Z., Kulawik, S. S., and Fischer, E. V.: PAN in the eastern Pacific free troposphere: A satellite view of the sources, seasonality, interannual variability, and timeline for trend detection, J. Geophys, Res.-Atmos., 122, 3614-3629, doi:10.1002/2016JD025868, 2017.

 Tables

661

662 Table 1. Chemical and meteorological characteristics of the four episodes.

	Episode 1	Episode 2	Episode 3	Episode 4
Period	Oct.31 ~ Nov.2	Oct. 28~29	Oct. 20~21	Nov. 4~5
Type	Transport dominant	Transport dominant	Chemical transformation	Chemical transformation
Event	O_3 export	O_3 export	Haze	Haze
O_3 (ppbv)	60.2 (80.6)	45.6 (62.8)	59.7 (78.9)	61.8 (87.5)
PAN (ppbv)	0.5 (0.9)	0.5 (0.8)	1.2 (2.0)	1.3 (2.4)
$PM_{2.5}$ ($\mu g/m^3$)	34 (62)	23 (36)	50 (76)	77 (156)
SO_2 (ppbv)	4.3 (12.9)	2.0 (4.4)	2.6 (5.4)	4.4 (9.5)
NO_2 (ppbv)	3.7 (7.3)	6.2 (12.1)	6.2 (12.7)	6.1 (9.9)
Wind Speed (m/s)	13.5 (16.0)	9.5 (16.1)	6.6 (10.2)	5.0 (7.7)

663 *Measurements are given for the average with the maximum in the parenthesis.

Figure Captions

Figure 1. Temporal variations (against local time) of measured species, including PAN, $PM_{2.5}$, O_3, NO_2, NO, SO_2, and, CO, and meteorological parameters, including relative humidity, temperature, and wind speed in fall 2010. Episodes 1–4, described in the main text, are shaded in blue and yellow.

Figure 2. Diurnal variations in the concentrations of O_3, NO_2, PAN, and $PM_{2.5}$, measured at GCO in the fall of 2010 (5 min data of O_3, NO_2, 2 min data of PAN, and 1 h data of $PM_{2.5}$).

Figure 3. Comparison of O_3 with the PAN daily maxima. The time when the daily maximum appears is classified as daytime (08–18 h) and nighttime (the rest) based on the time of sunrise and sunset. Numerals indicate the days.

Figure 4. The three-day NOAA HYSPLIT backward trajectories of air masses for every one hour observed at GCO during episode 1 (Oct. 31 to Nov. 2), episode 2 (Oct. 28–29), episode 3 (Oct. 20–21), and episode 4 (Nov. 4–5). They are colored according to the level of (a) PAN, (b) O_3, (c) NO_2, and (d) $PM_{2.5}$ at GCO at the time of the trajectory initialization. The trajectories north of 50°N are not shown. For these horizontal trajectories, (e) vertical heights are given.

Figure 5. Correlations between (a) PAN and O_3 and (b) PAN and NO_2 with linear regression line for each episode. Correlations between O_3 and PAN were color coded by the level of (c) NO_2 and (d) $PM_{2.5}$.

Figure 6. Correlations among PAN, K^+ ion of $PM_{1.0}$, and carbonaceous components of $PM_{2.5}$ for three cases: (a) PAN and $PM_{2.5}$ mass, (b) PAN and $PM_{2.5}$ OC, (d) $PM_{2.5}$ EC and OC, and (d) PAN and $PM_{1.0}$ K^+. The lines represent the linear regression for each episode.

Figure 7. Comparison between the observed and calculated (a) PAN and (b) O_3 concentrations by CAM-chem model. Time is given in local time and four episodes are shaded.
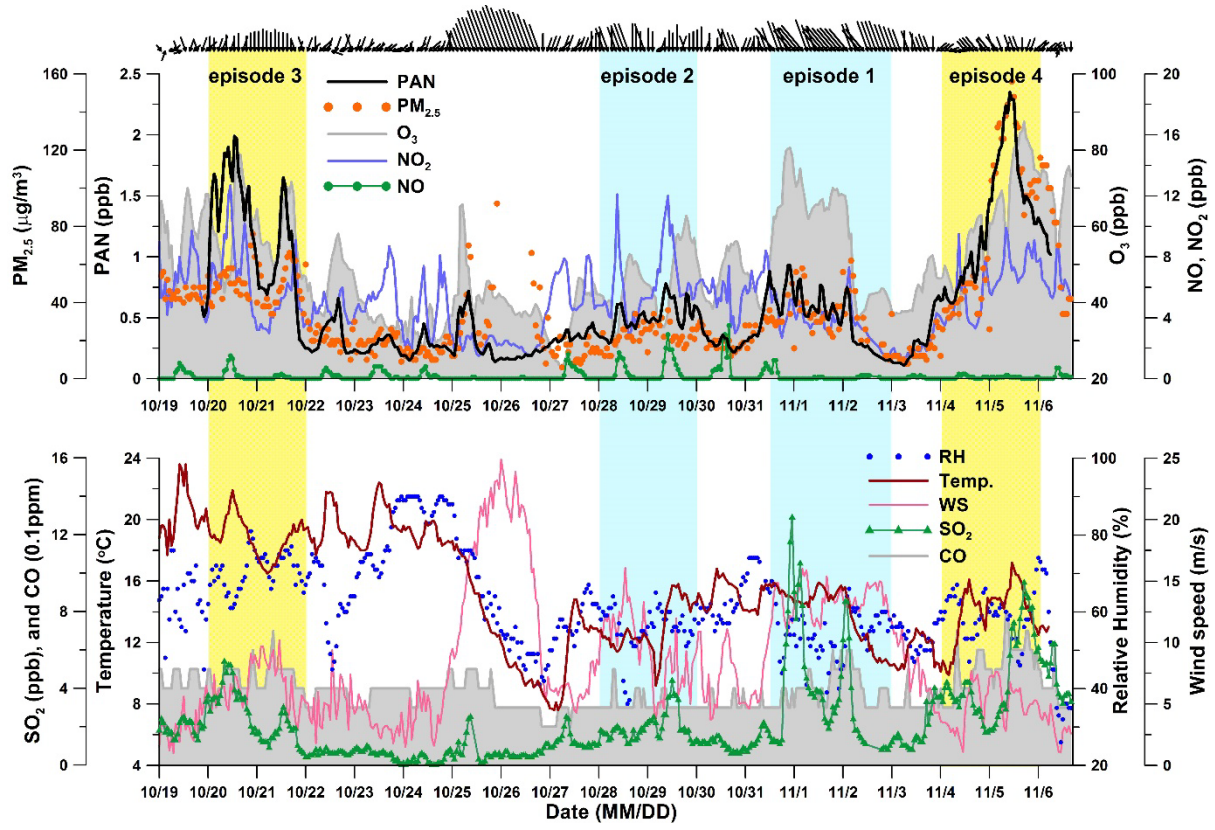
692
693   Figure 1.

694
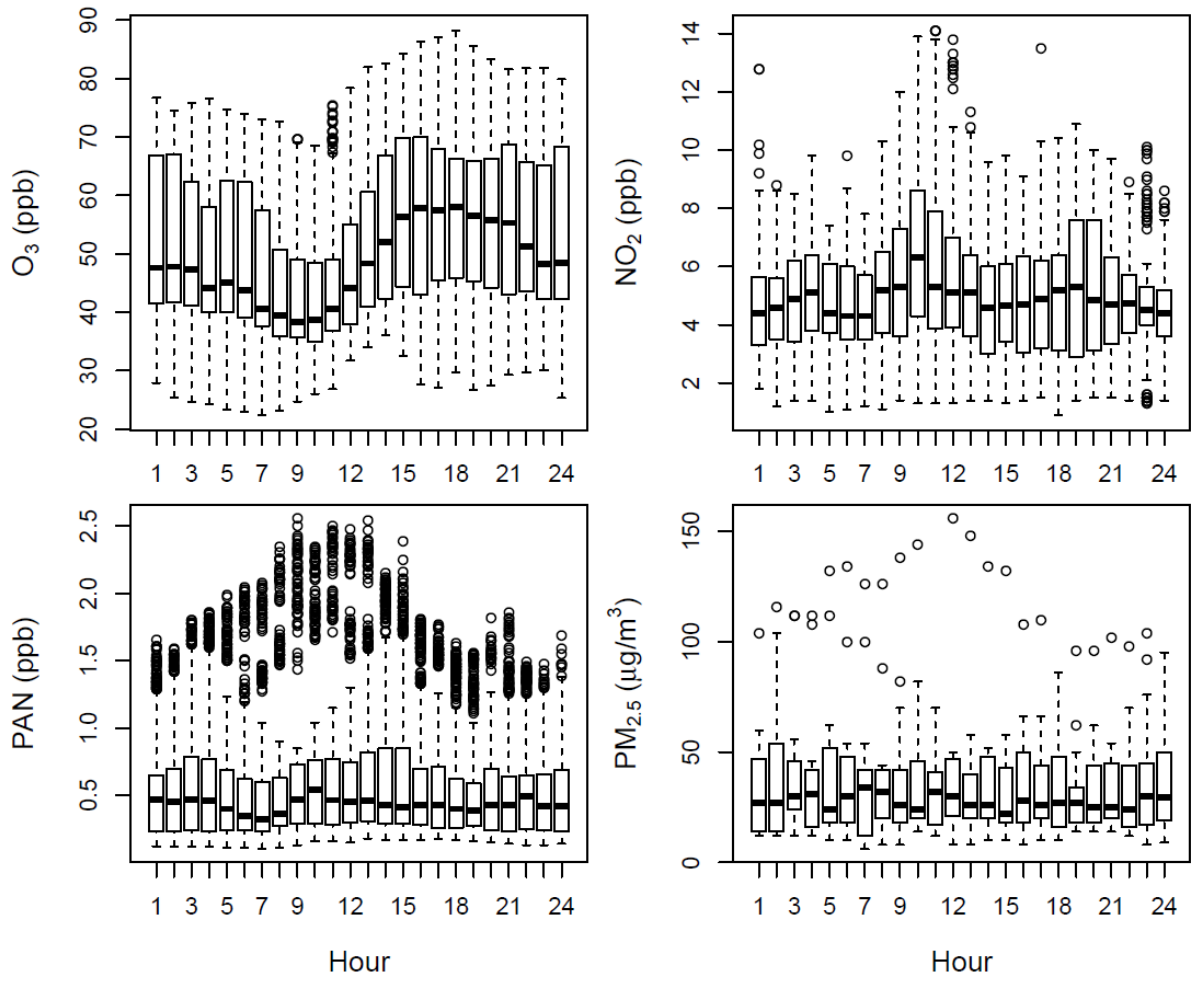
695

696   Figure 2.
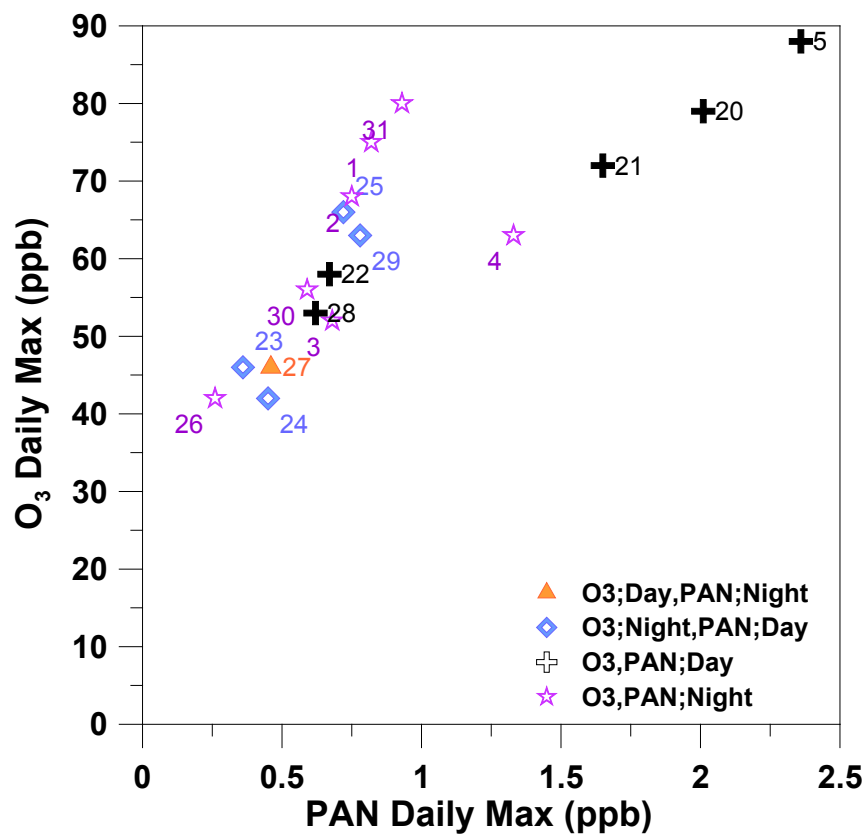
697

698   Figure 3.
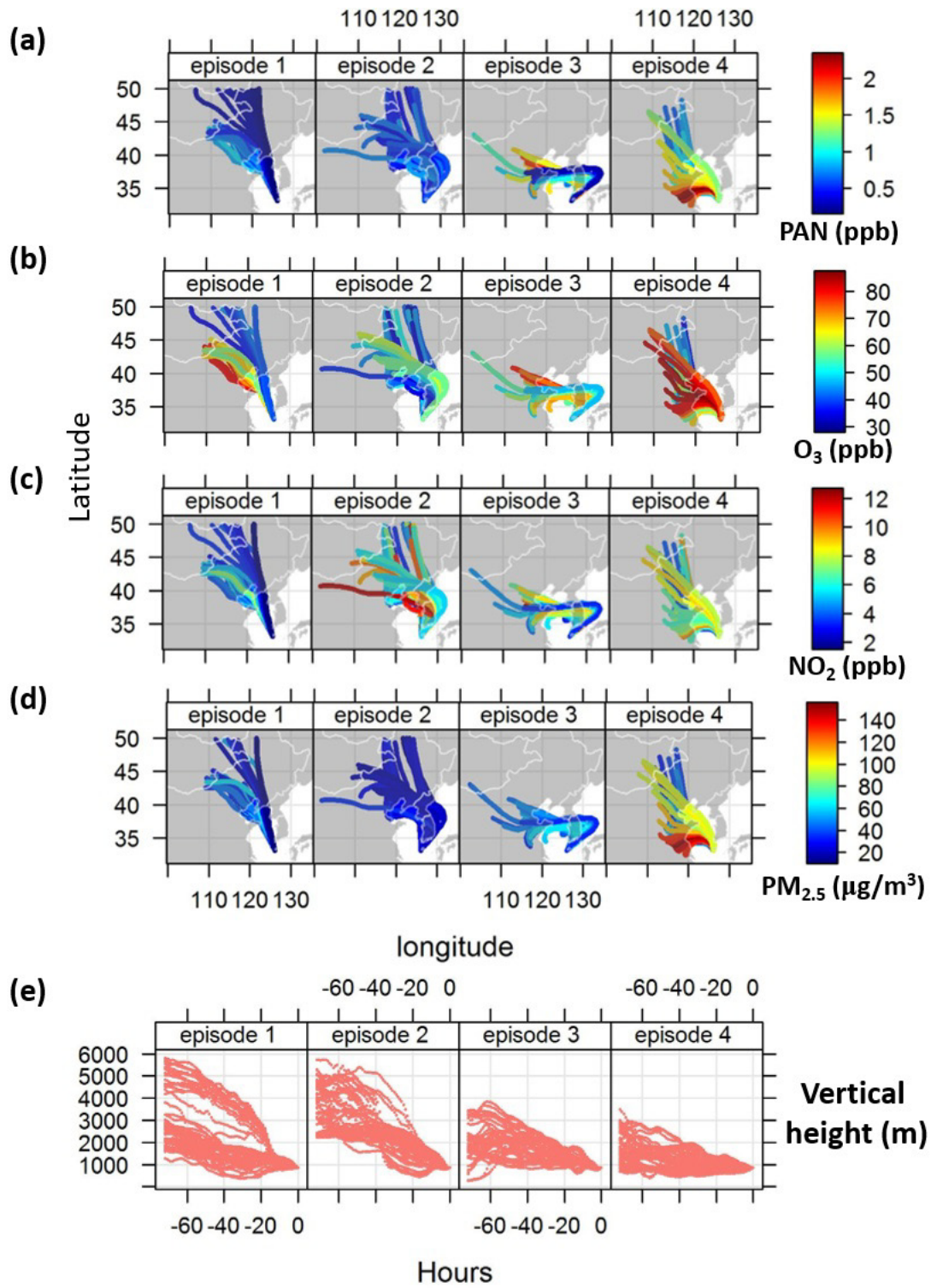
699

700   Figure 4.

701
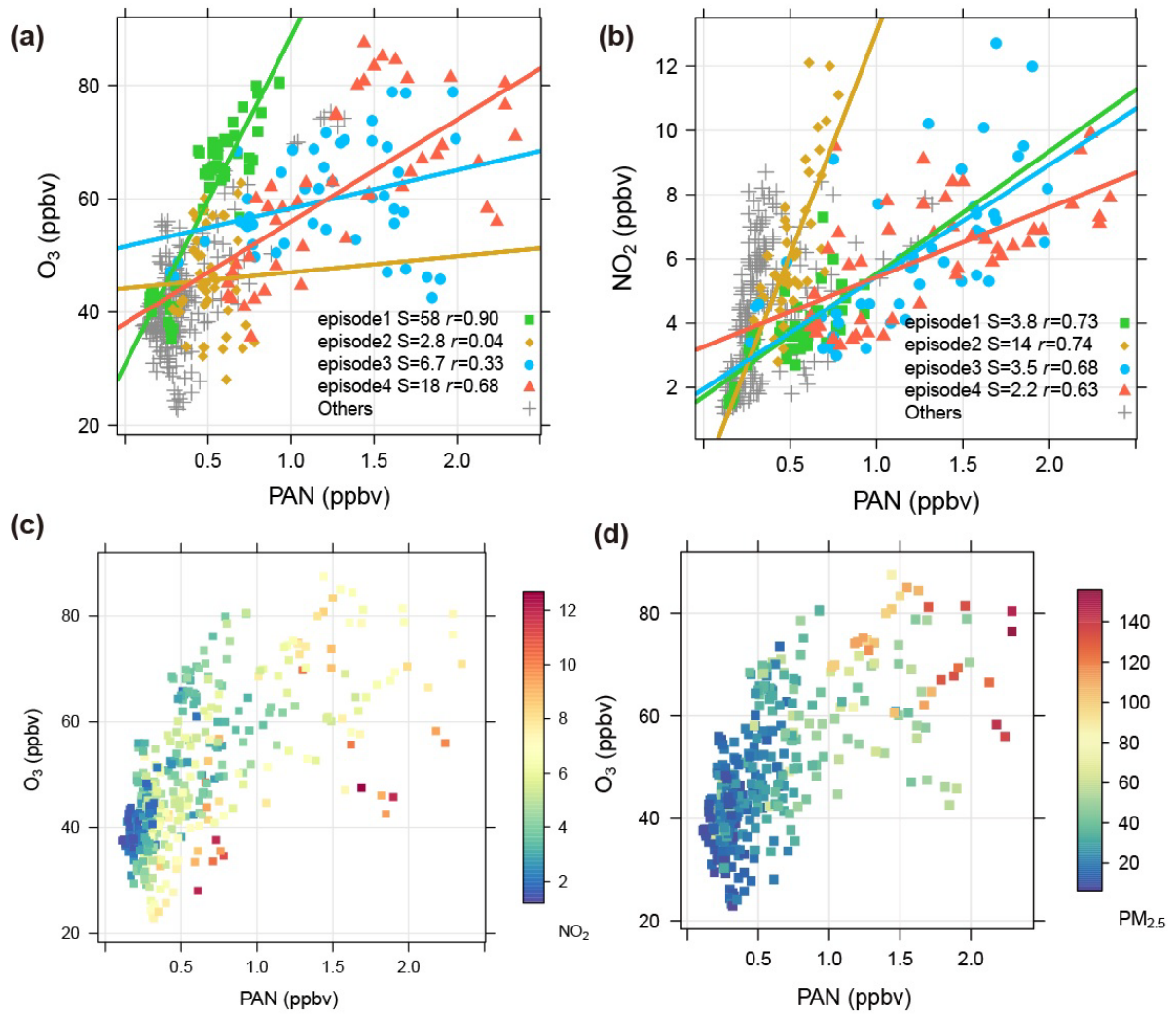
702

703   Figure 5.

704
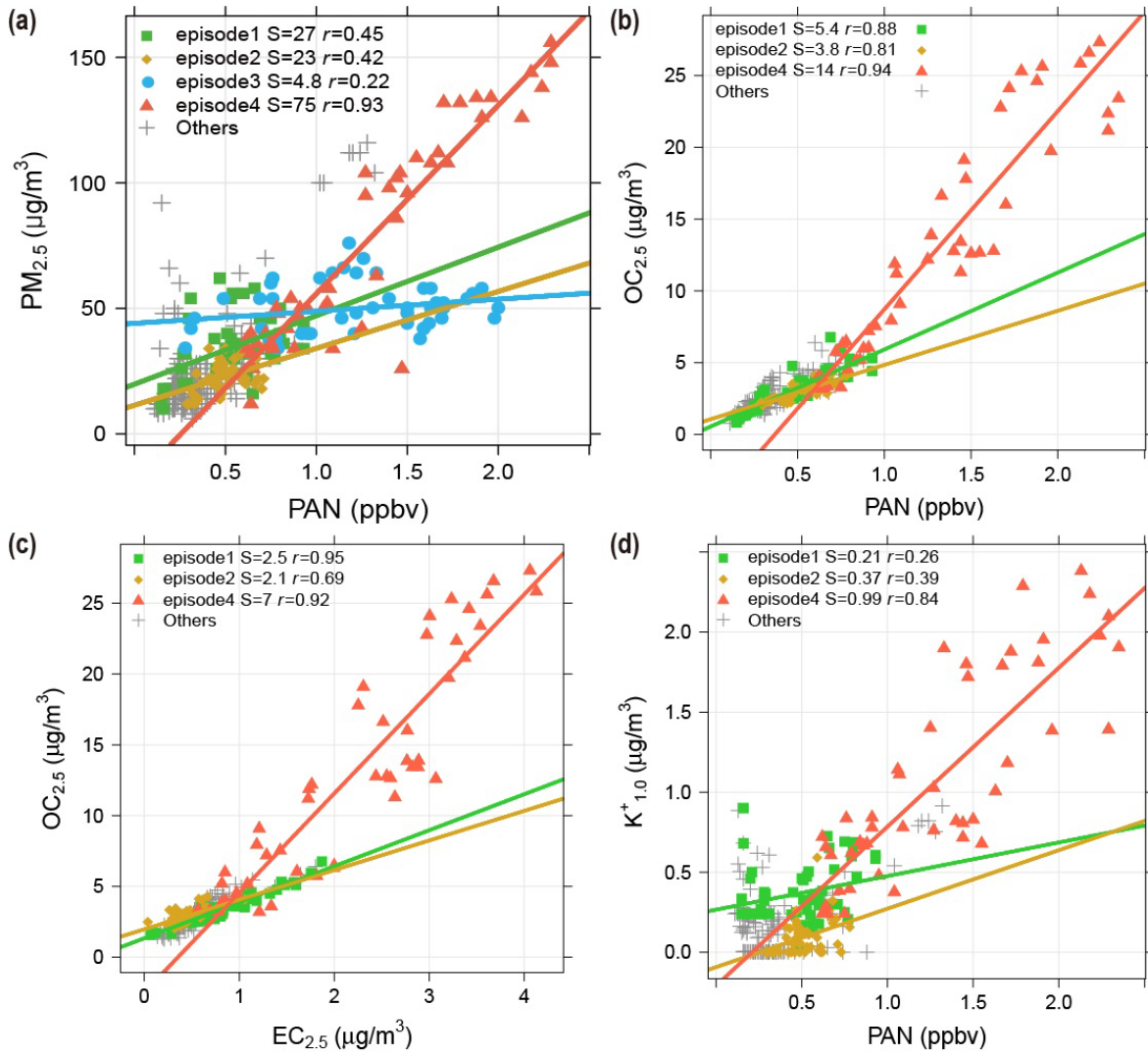
705

706   Figure 6.

707

708   Figure 7.